Numerical confirmation of skin-effect influence on RWM analysis

S. Mastrostefano[1], V. D. Pustovitov[2], Y. Liu[3], F. Villone[1]

[1] *Ass. Euratom/ENEA/CREATE, DIEI, Univ. di Cassino e del Lazio Meridionale, Italy*

[2] *Institute of Tokamak Physics, National Research Centre 'Kurchatov Institute', Russia*

[3] *Euratom/CCFE Fusion Association, Culham Science Centre, UK*

Introduction

Resistive Wall Modes (RWM) are usually treated as slow modes [1, 2, 3, 4] perfectly penetrating the vacuum vessel wall, so that the normal component of magnetic perturbations is assumed constant across the wall. In the theory of RWMs, this constitutes the widely used "thin wall" approximation [3, 4]. The advanced tokamak scenarios require operation quite above the stability limit [2, 3, 4], hence the mode growth rate can be so high (though still far below the Alfvenic level) that the standard RWM theory reviewed in [1, 3, 4] may not be valid because of the skin effect [5, 6]. The mode can be hence called "fast" RWM, being between the usual "slow" RWM and much faster ideal MHD modes on Alfvenic time scale.

We show evidence of the skin-effect modification of the Resistive Wall Mode (RWM) dynamics in a tokamak, using CarMa [7], a 3D volumetric code for the analysis of RMW. Contrary to other available three-dimensional RWM codes, like VALEN [8] or STARWALL [9], CarMa has the unique feature to combine the MHD models for the plasma with a volumetric treatment of the surrounding conductors, without resorting to the usual thin-wall approximation. This allows us to confirm the thick-wall effect predicted analytically in the cylindrical limit [5, 6]. The results prove that conventional thin-wall models may underestimate RWM growth rates.

Formulations

In the thin-wall models, the normal component of the magnetic field is assumed the same at the both sides of the wall. In the cylindrical approximation, calling $\tau_w = \mu_0 r_w d_w/\eta$ the wall time constant (r_w, d_w, η are the wall radius, thickness and resistivity, respectively), the dispersion relation for the RWM growth rate γ is:

$$\gamma\tau_w = \Gamma_m, \tag{1}$$

where Γ_m describes the plasma response. The thin-wall limit corresponds to $d_w/\delta \ll 1$, where $\delta = \sqrt{\eta/(\mu_0\gamma)}$ is the skin depth. In terms of γ, this means $\gamma\tau_w \ll r_w/d_w$. When the skin depth is only a small part of the wall thickness, the dispersion relation for the RWMs becomes [5, 6]:

$$\gamma\tau_w = \Gamma_m d_w/\delta. \tag{2}$$

Compared to (1), this gives larger growth rates. Also, since δ is a function of γ, this means a different dependence of γ on Γ_m:

$$\gamma\tau_w = \Gamma_m^2 d_w / r_w. \tag{3}$$

This indicates that the accuracy of the standard thin-wall approaches can be insufficient, when the skin depth becomes comparable with the wall thickness. Hence, reliable computational tools, able both to provide the correct growth rate scaling and to treat realistic geometries, are required. The CarMa code answers this need. A coupling surface S is introduced between the plasma and the conducting structures. Solving the linearized single-fluid MHD equations neglecting the plasma mass, the (instantaneous) plasma response matrix to magnetic field perturbations on S is computed and is coupled to a 3D volumetric integral formulation of the eddy currents problem, which describes the conducting structures by means of a three-dimensional finite elements mesh - no thin-wall approximation is made. The final form of the model [7] is:

$$L^* \frac{dI}{dt} + RI = 0, \tag{4}$$

where I is a vector of 3D discrete currents in the finite elements mesh, the fully populated inductance matrix L^* includes the plasma response, and the sparse matrix R describes the resistance of the 3D structures. The RWM growth rate γ is computed as the unstable eigenvalue of the dynamical matrix $-(L^*)^{-1}R$ of system (4).

Results

We refer to the circular plasma configuration described in [7] (major radius $R_0 = 2$m, minor radius $a = 0.4$m), for which the $n = 1$ external kink mode is unstable (n is the toroidal mode number). Several circular resistive walls are considered, with the same major radius R_0 and minor radii from $r_w = 1.3a$ to $r_w = 1.5a$; r_w denotes the position of the inner side of the wall. We consider geometrically thin walls with $d_w = r_w/10$, each described with a 3D finite elements discretization. The CarMa code can only treat thick walls; in order to reproduce the thin-wall approximation, we consider walls with $r_w/d_w \gg 1$, representing them with only one radial finite element in the wall width. After a suitable sensitivity analysis, we assume $r_w/d_w = 500$ as the thin-wall estimate.

Fig. 1 shows the growth rates for various wall configurations, both in the thin-wall approximation and using the full capacities of the CarMa code; also the thick-wall estimate (3) is reported. First of all, we notice that the thin-wall approximation fails to give a good estimate of the growth rate, except for low values of Γ_m. Secondly, CarMa is capable of reproducing the expected quadratic behaviour in terms of Γ_m, predicted by the thick-wall estimate (3) and

demonstrated in a simpler model without expansion in δ/d_w [10]. Figure 3 in [10] is , physically, equivalent to Fig. 1 here. The main difference is that it was obtained from Eq.(32) in [10] in the cylindrical approximation.

The thick-wall effect is expected to become significant when the skin depth δ is comparable to the wall width [5, 6, 10]. To verify this, we computed the quantity $\gamma\tau_w/\Gamma_m$ as a function of the ratio d_w/δ (Fig. 2). We refer here to the configuration with $r_w = 1.5a$, considering various walls of increasing thickness. When the penetration depth δ is much greater than the wall width d_w, we recover the thin-wall approximation, so that $\gamma\tau_w \to \Gamma_m$.When $d_w \simeq \delta$ (a situation in-between the validity range of the existing analytical models [5, 6, 10]) the error of the thin-wall approximation can exceed 50%. This proves the necessity of thick-wall calculations even at quite moderate growth rates and confirms the conclusions based on cylindrical calculations. The physical reason for the underestimation of the thin-wall approximation is twofold. First of all, the exponential attenuation of wall currents due to skin effect makes part of the wall ineffective in the stabilization, hence reducing the effective wall width. Secondly, the (stabilizing) magnetic field in the region outside the wall is reduced due to shielding of wall currents.

Since the models based on the thin-wall approximation can substantially underestimate the growth rate, when the wall width and the penetration depth become comparable, it is important to find possible equivalent simplified thin-wall modelling of thick structures. The first approach can be to fictitiously move the thin wall farther from the plasma with respect to its actual position. Fig. 3 reports the results obtained locating a thin wall at the geometrical barycenter of the thick wall, showing a substantial overestimation of the growth rate with respect to the reference computations. The second approach is to reproduce the 'true' thick-wall behaviour with multiple thin walls. Fig. 3 shows that, indeed, by using four nested thin walls we can substatially improve the agreement with the reference computation.

Conclusions

We have presented a confirmation, with a 3D RWM code, of the thick-wall effect recently predicted analytically in cylindrical geometry. The unique ability of the CarMa code of treating volumetric conductors has been exploited to highlight the limits of the usual thin-wall approximation, which underestimates the growth rate of RWM instability. The actual error becomes significant when the wall width and the penetration depth are comparable, which can occur in existing tokamaks for modes faster than conventional “slow" RWMs. This work was supported in parts by EFDA, by Italian MIUR under PRIN grant 2010SPS9B3 and by Rosatom State Corporation.

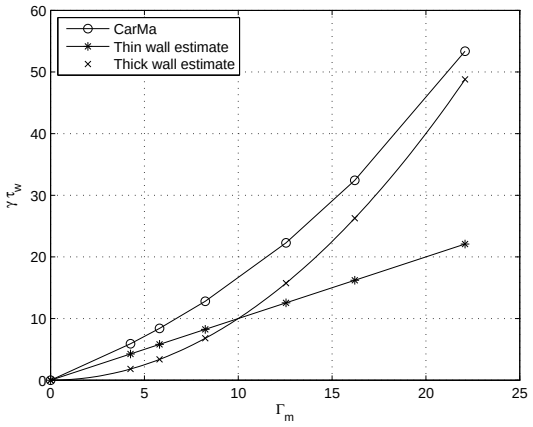

Figure 1: Growth rates comparison: thin wall vs. thick wall

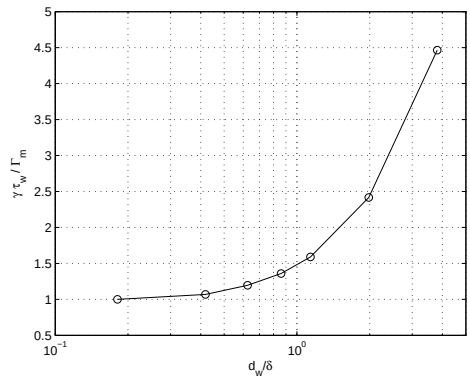

Figure 2: Scan of wall width

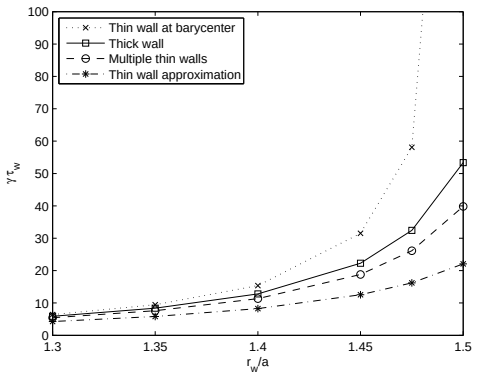

Figure 3: Growth rates with various wall models

References

[1] S. W. Haney and J. P. Freidberg, Phys. Fluids B **1** (1989) 1637

[2] E.J. Strait et al., Nucl. Fusion **43** (2003) 430

[3] T. C. Hender et al., Nucl. Fusion **47** (2007) S128

[4] M. S. Chu and M. Okabayashi, Plasma Phys. Controlled Fusion **52** (2010) 123001

[5] V. D. Pustovitov, Phys. Lett. A **376** (2012) 2001

[6] V. D. Pustovitov, Plasma Phys. Rep. **38** (2012) 697

[7] A. Portone, F. Villone et al., Plasma Phys. Controlled Fusion **50** (2008) 085004

[8] J. Bialek et al., Phys. Plasmas **8** (2001) 2170

[9] E. Strumberger et al., Phys. Plasmas **15** (2008) 056110

[10] V.D. Pustovitov, V.V. Yanovskiy, Plasma Phys. Rep. **39** (2013) 345